NEOPLASIA
www.neoplasia.com

Volume 12 Number 5 May 2010 pp. 376–387 376

Combination of Bifunctional Alkylating Agent and Arsenic Trioxide Synergistically Suppresses the Growth of Drug-Resistant Tumor Cells[1,2]

Pei-Chih Lee*,†, Rajesh Kakadiya†, Tsann-Long Su† and Te-Chang Lee*,†

*Institute of Pharmacology, School of Medicine, National Yang-Ming University, Taipei, Taiwan, Republic of China; †Institute of Biomedical Sciences, Academia Sinica, Taipei, Taiwan, Republic of China

Abstract

Drug resistance is a crucial factor in the failure of cancer chemotherapy. In this study, we explored the effect of combining alkylating agents and arsenic trioxide (ATO) on the suppression of tumor cells with inherited or acquired resistance to therapeutic agents. Our results showed that combining ATO and a synthetic derivative of 3a-aza-cyclopenta[*a*]indenes (BO-1012), a bifunctional alkylating agent causing DNA interstrand cross-links, was more effective in killing human cancer cell lines (H460, H1299, and PC3) than combining ATO and melphalan or thiotepa. We further demonstrated that the combination treatment of H460 cells with BO-1012 and ATO resulted in severe G_2/M arrest and apoptosis. In a xenograft mouse model, the combination treatment with BO-1012 and ATO synergistically reduced tumor volumes in nude mice inoculated with H460 cells. Similarly, the combination of BO-1012 and ATO effectively reduced the growth of cisplatin-resistant NTUB1/P human bladder carcinoma cells. Furthermore, the repair of BO-1012–induced DNA interstrand cross-links was significantly inhibited by ATO, and consequently, γH2AX was remarkably increased and formed nuclear foci in H460 cells treated with this drug combination. In addition, Rad51 was activated by translocating and forming foci in nuclei on treatment with BO-1012, whereas its activation was significantly suppressed by ATO. We further revealed that ATO might mediate through the suppression of AKT activity to inactivate Rad51. Taken together, the present study reveals that a combination of bifunctional alkylating agents and ATO may be a rational strategy for treating cancers with inherited or acquired drug resistance.

Neoplasia (2010) 12, 376–387

Introduction

DNA alkylating agents, commonly used as chemotherapeutic drugs for the treatment of a variety of pediatric and adult cancers [1], exert their cytotoxic effects by directly interacting with DNA in a way that leads to DNA lesions. There are two types of DNA alkylating agents, namely, monofunctional and bifunctional. Mechlorethamine, a bifunctional nitrogen mustard alkylating agent, was the first antitumor drug introduced into clinical practice more than 50 years ago [2]. Currently, a variety of bifunctional alkylating agents, such as the nitrogen mustards (e.g., melphalan [3]), nitrosoureas (e.g., carmustine [4]), alkyl sulfonates (e.g., busulfan [5]), aziridines (e.g., thiotepa [6]), platinum drugs (e.g., cisplatin [7]), and the natural product mitomycin C (MMC) [8], are still widely used for the treatment of patients with malignant diseases. Although monofunctional alkylating agents mainly form genotoxic monoadducts to further induce mutagenic and carcinogenic DNA lesions, bifunctional alkylating agents form monoadducts, intrastrand cross-links, and interstrand cross-links (ICLs) on DNA and also form DNA-protein cross-links [9]. ICLs cause replisome dissociation and collapse and, subsequently, induce DNA double-strand breaks (DSBs) [9,10]. The induction of ICLs by bifunctional alkylating agents therefore disturbs cell cycle progression and triggers cell death. Because the repair of ICLs is a

Address all correspondence to: Te-Chang Lee, PhD, Institute of Biomedical Sciences, Academia Sinica, Taipei, Taiwan 11529, ROC. E-mail: bmtcl@ibms.sinica.edu.tw

[1]This work was supported by Academia Sinica (grant no. AS-96-TP-B06). No potential conflicts of interest are disclosed.

[2]This article refers to supplementary materials, which are designated by Figures W1 to W3 and are available online at www.neoplasia.com.

Received 5 January 2010; Revised 23 February 2010; Accepted 25 February 2010

DOI 10.1593/neo.10110

laborious challenge compared with other DNA damages, the formation of ICLs is the critical step in the cytotoxicity of bifunctional alkylating agents and is recognized as a critical event in targeting cancer therapies [9]. On the basis of MMC and bis(carbamates)-pyrrolizidines, we previously synthesized a series of bifunctional alkylating agents, bis(hydroxymethyl) of 3a-azacyclopenta[*a*]indene-1-yl, and their bis(methylcarbamate) derivatives, and showed potent anticancer activity in a variety of *in vitro* cell models and *in vivo* xenograft mouse models [11]. Among the series of 3a-aza-cyclopenta[*a*]indenes, BO-1012 (Figure 1*A*) induced a significant level of ICLs and suppressed the growth of human breast carcinoma cells transplanted in nude mice [11].

Arsenic trioxide (ATO) is an antineoplastic chemotherapeutic agent approved for treatment of relapsed or refractory acute promyelocytic leukemia [12]. ATO has also been reported to reduce cell viability, induce apoptosis, and inhibit tumor growth in myeloma cells at concentrations low enough for safe use in patients [13]. Recent studies have further demonstrated that ATO is highly effective for

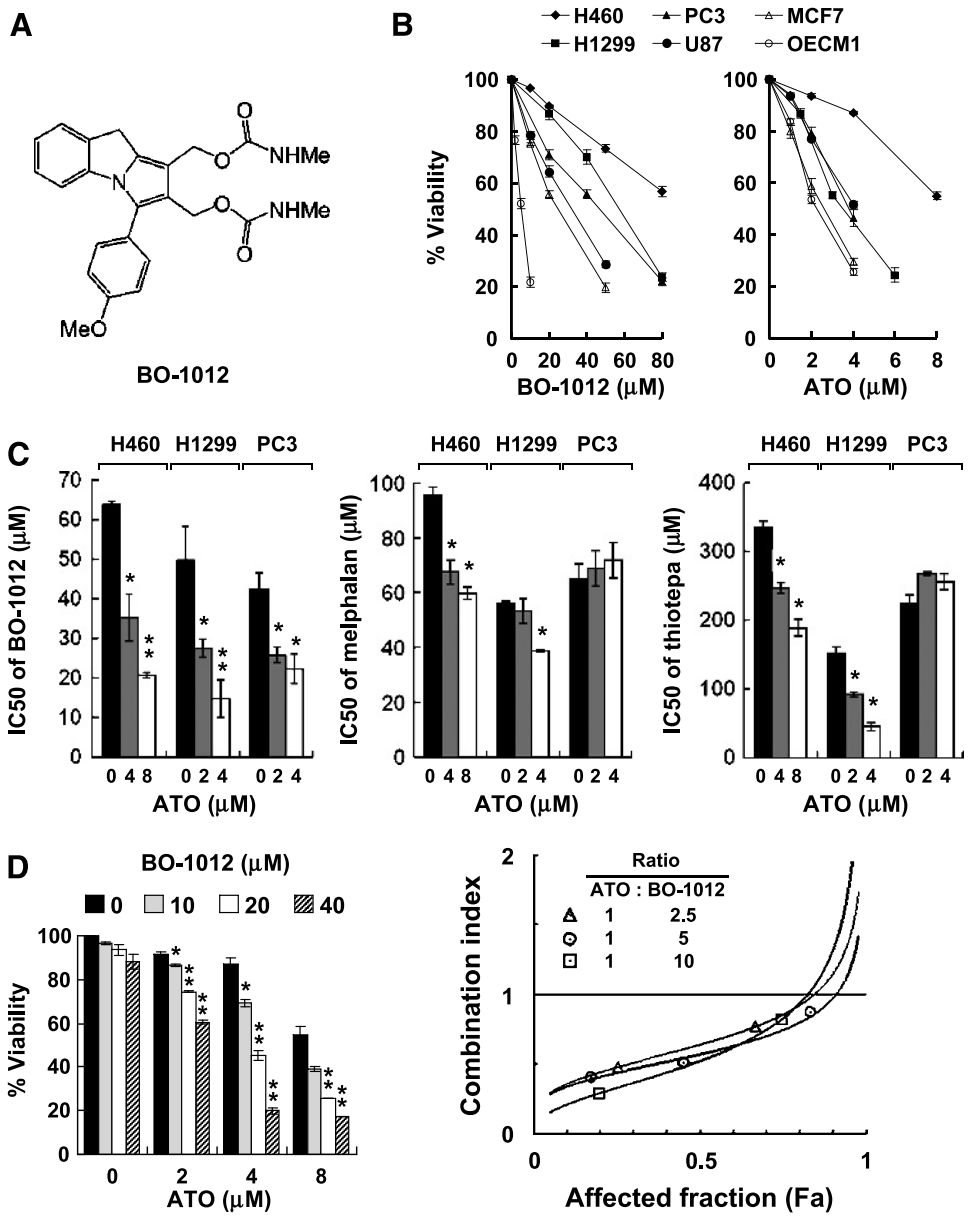

Figure 1. Enhanced cytotoxicity of BO-1012 by ATO in human cancer cell lines. (A) Chemical structure of BO-1012. (B) Cytotoxicity of human cancer cell lines to BO-1012 and ATO. Six human cancer cell lines, H460, H1299, PC3, U87, MCF7, and OEC-M1, were treated with various concentrations of BO-1012 or ATO for 72 hours. Cell viability was determined by the WST-1 assay. (C) Enhanced cytotoxicity of BO-1012, melphalan, and thiotepa by ATO cotreatment in three relatively resistant cell lines. Three relatively resistant cells, H460, H1299, and PC3, were exposed to ATO with BO-1012, melphalan, or thiotepa for 72 hours. The cell viabilities and IC_{50} values of BO-1012 and other two bifunctional alkylating agents in combination with or without ATO were calculated. $^{*}P < .05$, $^{**}P < .001$, compared with the IC_{50} values of each bifunctional alkylating agent alone. (D) Synergistic cytotoxicity of BO-1012 and ATO in H460 cells. H460 cells were treated with BO-1012 for 1 hour, washed, and then treated with ATO for 72 hours. Left: Cell viability analysis was performed. $^{*}P < .05$, $^{**}P < .001$ compared with the viability of cells treated with ATO alone. Right: The isobologram analysis of CI against affected fraction (Fa) was obtained by constant ratio combination method as described in Materials and Methods.

triggering apoptosis *in vitro* in a variety of solid tumor cells and for inhibiting tumor growth in xenograft animal models [14]. The promising preclinical activity of ATO against solid tumors supports further investigation of clinical applications for ATO. However, preliminary reports from phase 2 clinical trials on patients with metastatic renal cell carcinoma [15] and metastatic melanoma [16] suggest that ATO used as a single therapeutic agent may have limited efficacy against solid tumors.

Alternatively, numerous reports have shown that ATO can be used in combination with agents that induce apoptosis [17–19], reduce glutathione [18], inhibit DNA methylation [20], or induce DNA damage [21]. ATO also enhances radiosensitivity to human cervical carcinoma and malignant glioma cells *in vitro* and *in vivo* by enhancing autophagic effects and preventing tumor invasion [21–25]. Moreover, a phase 2 trial of ATO in combination with melphalan and ascorbic acid against myeloma showed that the addition of ATO and ascorbic acid to high-dose melphalan is safe and well tolerated in patients with relapsed or refractory multiple myeloma [23]. Therefore, combined treatment using ATO and other anticancer agents may have the potential to treat malignant tumors both effectively and safely.

Our early studies and others have reported that arsenic compounds synergistically enhance the cytotoxicity of UV and x-ray irradiation, DNA alkylating agents, and cross-linking agents [21,24–26]. Numerous studies have shown that arsenic inhibits activity of proteins involved in DNA repair by various mechanisms [27,28] and interferes with both base excision repair and nucleotide excision repair [29]. ATO is likely to enhance the cytotoxicity of DNA-damaging agents by inhibiting DNA repair [26]. Therefore, the combination of ATO and DNA-damaging agents such as bifunctional alkylating agents is anticipated to synergistically suppress tumor growth. Because drug resistance, both inherited and acquired, is a pervasive problem and is a key factor contributing to the failure of clinical chemotherapy, it is of vital importance to develop a regime against cancers that are resistant to chemotherapeutic agents. In this study, we conducted preclinical experiments to demonstrate that the combination of BO-1012 and ATO provides an effective strategy against tumor cells with inherited and acquired drug resistance *in vitro* and suppresses their growth in xenograft mouse models.

Materials and Methods

Reagents and Chemicals

BO-1012 was synthesized in a four-step reaction as described previously [11]. ATO and other reagents were purchased from Merck (Darmstadt, Germany), and melphalan and thiotepa were from Sigma-Aldrich (St Louis, MO). Chemicals for cell culture were obtained from Gibco (Grand Island, NY), and fetal bovine serum was from HyClone (Logan, UT).

Cell Lines and Cell Culture

H460 (human lung large cell carcinoma cells), H1299 (human non–small cell lung carcinoma *p53*-deficient cells), PC3 (human prostate carcinoma cells), U87 (human glioma cells), and MCF7 (human breast carcinoma cells) were purchased from the American Type Culture Collection (Rockville, MD). OEC-M1 (human gingival squamous cell carcinoma cells) was obtained from Dr C.-L. Meng (National Defense Medical College, Taiwan) [30]. NTUB1 (human bladder transitional carcinoma cells) and the cisplatin-resistant subline NTUB1/P were provided by Dr Y.-S. Pu (National Taiwan University Hospital, Taiwan) [31,32]. All cell lines (except U87, which was grown in minimum essential medium) were cultured in RPMI 1640 medium supplemented with 10% fetal bovine serum and antibiotics and were incubated at 37°C in a humidified atmosphere with 5% CO_2.

Measurement of Cell Viability

Cell viability was assessed using the cell proliferation reagent WST-1 (Roche Molecular Biochemicals, Penzberg, Germany), which is a tetrazolium salt that is cleaved by mitochondrial dehydrogenase in viable cells. In brief, 2000 to 7000 cells were seeded in each well of 96-well plates and were incubated at 37°C overnight before drug treatment. After a 72-hour incubation with BO-1012 alone (~0.1-80 μM), ATO alone (~1-8 μM), or BO-1012 plus ATO, WST-1 solution was added to each well at a 1:10 dilution, and cells were incubated at 37°C in 5% CO_2 for 4 hours. Cell viability was assessed by absorbance at 460 nm using an automatic ELISA plate reader. The values of 50% inhibition concentration (IC_{50}) for each drug were determined from dose-effect relationship at six or seven concentrations of each drug using the CompuSyn software (version 1.0.1; CompuSyn, Inc, Paramus, NJ) by Chou and Martin based on the median-effect principle and plot. The interactions between ATO and BO-1012 were evaluated by the Chou-Talalay combination indices (CIs) [33,34], where CI < 1 indicates synergy; CI = 1, additivity; and CI > 1, antagonism.

Modified Single-Cell Gel Electrophoresis (Comet) and DNA ICL Repair Assays

The formation and the repair of DNA ICLs in H460 cells were analyzed using a modified comet assay as described previously [11].

Cell Cycle Analysis

H460 cells were treated with BO-1012 and ATO, separately or in combination, as described above. Cell cycle analysis was performed as described previously [35]. In brief, at the end of treatment, the attached cells were trypsinized, fixed with ice-cold 70% ethanol, stained with 4 μg/ml propidium iodide in PBS containing 1% Triton X-100 and 0.1 mg/ml RNase A, and then subjected to flow cytometric analysis (FACScan flow cytometer; Becton Dickinson, San Jose, CA). The cell cycle phase distribution was analyzed using ModFit LT 2.0 software (Verity Software House, Topsham, ME).

Measurement of Histone H2AX Phosphorylation

After treatment with BO-1012, ATO, or a combination of both agents for 24, 48, or 72 hours, cells were fixed with 70% ethanol for 16 hours, washed with PBS, and incubated with mouse anti-γH2AX antibody (Upstate, Biotechnology, Lake Placid, NY) for 2 hours, followed by fluorescein isothiocyanate–conjugated goat antimouse (Jackson ImmunoResearch Laboratories, West Grove, PA) for 30 minutes. Cells were then stained in PBS containing 4 μg/ml propidium iodide and 0.1 mg/ml RNase A and were analyzed with a FACScan flow cytometer. γH2AX-labeled cells were gated according to control histograms, and their percentage in a total of 10,000 cells was calculated for each treatment.

Immunofluorescence Staining

H460 cells were cultured onto slides and then treated with BO-1012 and ATO, separately and in combination as described above. To visualize γH2AX or Rad51, cells were washed with cold PBS and

fixed with 100% ice-cold methanol for 30 minutes. Slides were washed with PBS and incubated with anti-γH2AX for 2 hours or anti-Rad51 antibody for 4 hours at room temperature followed by Alexa Fluor 488 or 555–conjugated secondary antibodies (Molecular Probes, Eugene, OR), respectively, and 4′-6-diamidino-2-phenylindole (DAPI). After mounting with 50% glycerol, slides were subjected to confocal image analysis (Radiance 2100 System; Bio-Rad, Hertfordshire, England). Cells with at least four γH2AX foci in nuclei were counted manually as positive.

Apoptosis Assays

H460 cells were exposed to BO-1012, ATO, or a combination of both agents, and then apoptosis was detected by flow cytometry using the annexin V–FITC Apoptosis Detection Kit (Calbiochem, La Jolla, CA) according to the manufacturer's instructions. In the annexin V flow cytometry assay, the cells positive for annexin V staining only (*bottom right quadrant*) and positive for both annexin V and DNA staining (*top right quadrant*) represent the early and late apoptotic populations, respectively. The cells positive for DNA staining only (*top left quadrant*) represent the necrotic population.

Xenograft Mouse Model and Therapy

Animal care was approved by and followed the guidelines of the Academia Sinica Institutional Animal Care and Utilization Committee. Male Balb/c nude mice 6 weeks of age were obtained from the National Laboratory Animal Center (Taipei, Taiwan). The animals were housed in a specific pathogen-free environment under controlled conditions of light and humidity and were given sterilized food and water *ad libitum*. They were allowed to acclimate for 48 hours after shipment before tumor inoculation was carried out. H460 (3×10^6 cells), NTUB1 (1×10^7 cells), or NTUB1/P (1×10^7 cells) cells in 50 μl of PBS, pH 7.4, were inoculated subcutaneously into the hind limb of mice. When the resulting tumors reached 80 to 100 mm^3 in diameter, mice were randomly assigned to different treatment groups. ATO (5 mg/kg body weight), BO-1012 (2.5 mg/kg), or a combination of both agents was injected intravenously five times daily. BO-1012 solution was prepared in 20% DMSO and 15% Tween 80 in 0.9% saline, whereas ATO was dissolved in 4N NaOH, diluted in 0.9% saline and neutralized with 1N HCl before injection. To monitor tumor formation, the longest and shortest diameters of the tumors were measured using calipers. Tumor volume (mm^3) was calculated according to the following formula: tumor volume = (length × width^2) / 2. Mouse body weight was also measured every 2 to 3 days and used as an indicator of the systemic toxicity of the treatment.

Terminal Deoxynucleotidyl Transferase-Mediated dUTP Nick End Labeling Assay

The terminal deoxynucleotidyl transferase-mediated dUTP nick end labeling (TUNEL) assay was performed to quantify apoptotic cells in xenograft tumor sections using the Dead End kit (Promega, Madison, WI) with the assistance of an autostainer (Dako, Carpinteria, CA). The assay was carried out according to the manufacturer's instructions.

Immunohistochemical Staining

Immunohistochemical analysis of proliferating cell nuclear antigen (PCNA) was conducted on established tumors from mice 1 day after treatment. One day after the last injection with drugs (day 6), three mice from each group were killed, and tumors were sectioned and then stained with anti-PCNA antibody (PC-10, mouse immunoglobulin G; DakoCytomation, Carpinteria, CA). The standard immunohistochemical staining was then performed according to the manufacturer's instructions of LSAB2 streptavidin-biotin complex system (Dako Corp).

Western Blot Analysis

Nuclei were isolated from H460 cells using Nuclei EZ Prep Nuclei Isolation Kit (Sigma). Rad51, DNA-PKcs, phospho-AKT, and AKT were analyzed by Western blot analysis technique as described previously [30].

Statistical Analysis

All data represent at least three independent experiments. The data are presented as means ± SE. The statistical significance of differences was assessed using the Student's *t*-test.

Results

Human Solid Tumor Cells with Inherited Resistance Were Sensitive to the Combination of BO-1012 and ATO

We recently reported that BO-1012 exhibits potent anticancer activity against human lymphoblastic leukemia and various solid tumors *in vitro* and against tumor xenografts *in vivo* [11]. In this study, we first investigated whether ATO could sensitize human solid tumor cell lines to BO-1012–induced cell death. Six tumor cell lines (H460, H1299, PC3, U87, MCF7, and OEC-M1) were treated with various concentrations of BO-1012 (~0.1-80 μM) or ATO (~1-8 μM) for 72 hours. The inhibitory effect of BO-1012 against these tumor cell lines covered a wide range, with IC_{50} values ranging from 5.2 μM (OEC-M1 cells) to 63.8 μM (H460 cells). OEC-M1 and MCF7 cells were highly susceptible to BO-1012, whereas H460, H1299, and PC3 cells were more resistant (Figure 1*B*). Similarly, ATO was significantly more cytotoxic to OEC-M1 and MCF7 cells than to H460 cells (Figure 1*B*).

To overcome the inherited resistance of H460, H1299, and PC3 cells to BO-1012 and ATO, the tumor cell lines were cotreated with ATO in combination with BO-1012 for 72 hours. The cytotoxic effects of combination of ATO and two clinically chemotherapeutic drugs, melphalan and thiotepa, were also investigated for comparison. The IC_{50} values of BO-1012 were significantly reduced by cotreatment with ATO, suggesting that the cytotoxicity of BO-1012 to these inherited resistance cell lines was synergistically enhanced by combining BO-1012 and ATO (Figure 1*C*). Synergistically cytotoxic effects were observed only in certain combinations of ATO and melphalan or thiotepa in H460 cells and H1299 cells and not in PC3 cells (Figure 1*C*). Apparently, the combination of BO-1012 and ATO was more effective in killing cancer cells than the combination of the other two drugs and ATO. Furthermore, cotreatment of three bifunctional alkylating agents with ATO showed no synergistic cytotoxic effect in susceptible cell lines such as OCE-M1 and MCF7 cells (data not shown).

Because H460 cells were the most resistant to BO-1012 and ATO, they were used to study further the synergistic effects of these two agents. As shown in Figure 1*D*, treatment of H460 cells with 0 to 40 μM BO-1012 for 1 hour did not significantly reduce the cell growth rate; however, cell viability decreased substantially when BO-1012–treated H460 cells were subsequently exposed to ATO (0-8 μM) for 72 hours. The interactions between ATO and BO-1012 were evaluated by the Chou-Talalay CIs [33]. The CIs in all treatments were less than 1 (Figure 1*D*), confirming that treatment with BO-1012 and ATO had a synergistic cytotoxic effect.

ATO Prolongs the Duration of Cell Cycle Perturbation Induced by BO-1012 in H460 Cells

Because DNA-damaging agents may result in the inhibition of cell cycle progression, we investigated the effects of BO-1012, ATO, and a combination of both agents on cell cycle progression in H460 cells. After the treatment of H460 cells with 10 or 20 μM BO-1012 for 1 hour and subsequent treatment with 8 μM ATO for various periods, the cell cycle distribution was analyzed using a flow cytometer. As shown in Figure 2*A*, 8 μM ATO alone showed a minimal effect on the cell cycle distribution compared with the untreated control, whereas BO-1012 treatment significantly disturbed cell cycle progression. At the concentrations used, BO-1012 treatment resulted in the accumulation of cells in the S phase at 24 hours and in the G_2/M phase at 48 hours, and then the cell cycle distribution reverted to the same as seen in the control at 72 hours. When BO-1012–treated H460 cells were posttreated with ATO, significant S and G_2/M arrests were noticeable at 48 and 72 hours, respectively. We infer that the effect of ATO is mediated by inhibiting the repair of BO-1012–induced DNA damage, resulting in prolonged cell cycle delay.

BO-1012 Cooperates with ATO to Augment Induction of Annexin V$^+$ Cells

Apoptosis is usually triggered by DNA damage and cell cycle disturbance. Furthermore, ATO alone has been shown to induce apoptosis [36]. We therefore examined whether BO-1012 induces apoptosis, and whether this effect could be enhanced by posttreatment with ATO. After treatment of H460 cells with BO-1012 for 1 hour followed by ATO treatment for 24, 48, and 72 hours, an annexin V apoptosis assay was performed, and the percentage of annexin V$^+$ cells was determined by flow cytometry. Figure W1 shows a representative flow cytometry histogram of apoptosis. The annexin V$^+$ cells in the *top right* and *bottom right quadrants* indicate late and early apoptosis, respectively. As shown in Figure 2*B*, the combination of BO-1012 at 10 or 20 μM with ATO at 8 μM was much more effective in inducing annexin V$^+$ cells than either agent alone.

BO-1012 with ATO Inhibits Tumor Growth in Mice Bearing H460 Tumor Xenografts

The synergistic cytotoxic effect of BO-1012 with ATO in cultured cells drew us to investigate the potential benefit of combining BO-1012 and ATO against inherited resistance H460 cells in a xenograft animal model. H460 cells were subcutaneously inoculated into the hind limb of nude mice. After tumor formation, the mice were treated daily with 2.5 mg/kg BO-1012 and/or 5 mg/kg ATO through intravenous (i.v.) injection for 5 days. As shown in Figure 3*A*, the combined treatment of BO-1012 and ATO significantly suppressed the growth of H460 tumors in nude mice by ~82% (on day 25). BO-1012 and ATO combination treatment induced an obvious tumor growth delay, requiring 23.3 days to achieve a tumor volume of 500 mm^3, compared with 7, 7.1, and 9.4 days in untreated control, ATO alone, and BO-1012 alone groups, respectively (Figure 3*A*).

At the end of the experiments (on day 25), the tumor size and weight were determined when the animals were killed. As shown in Figure 3*B*, tumor size and weight were synergistically reduced in animals treated with a combination of BO-1012 and ATO compared with those treated with BO-1012 or ATO alone. The mouse body weight loss, commonly used to evaluate systemic toxicity induced by treatment, was less than 6% in animals treated with BO-1012 alone or BO-1012 plus ATO (Figure 3*C*). These results indicate that BO-1012 and its combination with ATO did not cause obvious systemic toxicity.

To further examine the anticancer effects of the combination of BO-1012 with ATO, we performed histopathologic evaluation 24 hours after the last treatment (i.e., day 6). Using an apoptosis marker level determined by the TUNEL assay, apoptosis was significantly increased in tumors treated with a combination of BO-1012 and ATO. Furthermore, the cell proliferation marker PCNA was markedly suppressed (Figure 3*D*). These results indicate that combined treatment of BO-1012 and ATO not only induced apoptotic cell death but also inhibited tumor cell growth substantially.

Combination of BO-1012 with ATO Overcomes Cisplatin-Resistant Bladder Urothelial Carcinoma In Vitro *and* In Vivo

In addition to the cells with inherited drug resistance such as H460, we also studied the anticancer effects of BO-1012 in combination with ATO against cells with acquired drug resistance. NTUB1/P cells, derived from the human bladder urothelial carcinoma cell line NTUB1 [31], are 60-fold more resistant to cisplatin than the parental cells [32]. We confirmed that the IC_{50} values of cisplatin in NTUB1 and NTUB1/P were 3.6 and 211.7 μM, respectively. Besides, we also found that the IC_{50} values of BO-1012 alone against NTUB1 and NTUB1/P were 24.8 and 85.4 μM; and the IC_{50} values of ATO alone were 0.4 and 3.8 μM, respectively. Thus, NTUB1/P cells were 3.4- and 9.5-fold more resistant than NTUB1 cells to BO-1012 and ATO, respectively. Using the same treatment protocol as described in Figure 1*D*, we observed that there was a synergistic effect on the inhibition of cell growth in cultures of NTUB1/P cells (Figure 4*B*; the range of CI values was 0.7-0.58) but not NTUB1 cells (Figure 4*A*; the range of CI values was 1.2-1.3). To confirm the anticancer activity of this combination in an animal model, we treated nude mice bearing NTUB1 or NTUB1/P xenografts with 2.5 mg/kg BO-1012 and/or 5 mg/kg ATO (i.v. injection five times daily). ATO alone did not effectively suppress the growth of either NTUB1 or NTUB1/P tumors in nude mice (Figure 4, *C* and *D*, respectively). In contrast, NTUB1 tumors were nearly completely suppressed by BO-1012, but only a 55% reduction in tumor volume was observed in mice bearing NTUB1/P xenografts. Remarkably, using a combination of BO-1012 and ATO at the same doses, more than 92% reduction of NTUB1/P tumor volume was achieved. These results indicated that BO-1012 alone was effective against tumor growth of drug-sensitive NTUB1 cells, whereas the combination of BO-1012 and ATO was required for suppressing the growth of drug-resistant NTUB1/P cells.

Repair of BO-1012–Induced DNA ICLs Is Inhibited by ATO

Whereas ATO is known to regulate DNA repair pathways, experiments were conducted to understand whether ATO interferes with repair of DNA ICLs induced by BO-1012. Using the alkaline gel shift assay, we confirmed that BO-1012, similar to melphalan and thiotepa, can interact with DNA to form ICLs *in vitro* (Figure W2). A modified comet assay was thus adopted to investigate the formation of ICLs in H460 cells treated with BO-1012 and ATO. As shown in Figure 5*A*, ICLs increased in a dose-dependent fashion in H460 cells treated with BO-1012, melphalan, or thiotepa for 1 hour. BO-1012 induced higher levels of ICLs than melphalan or thiotepa. ATO alone did not cause ICLs (data not shown). However, posttreatment of BO-1012–treated H460 cells with ATO significantly delayed the repair of

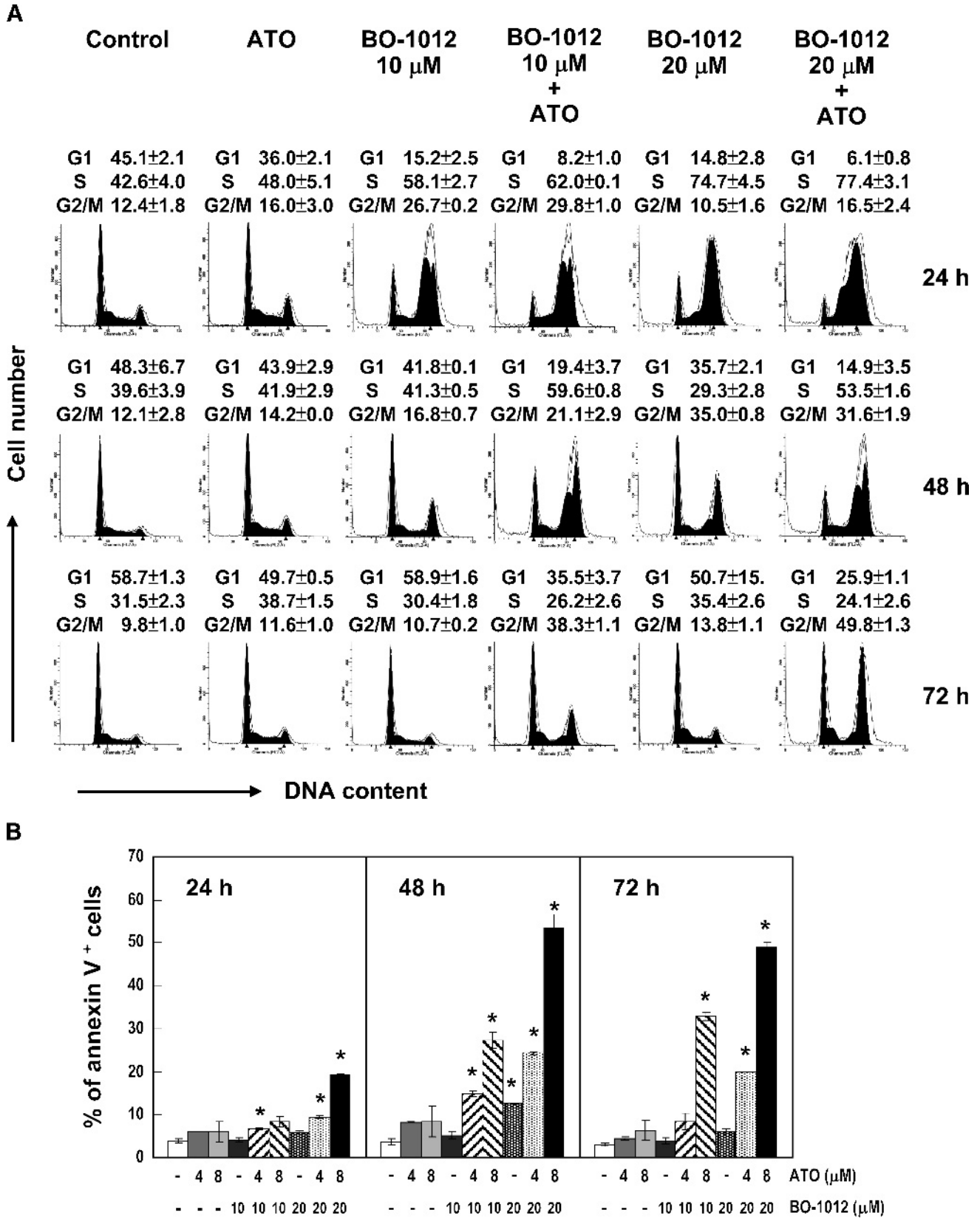

Figure 2. Cell cycle perturbation and apoptotic cell death induced by BO-1012, ATO and in combination. H460 cells were treated with 10 or 20 μM BO-1012 for 1 hour, washed, and then treated with 8 μM ATO for 24, 48 or 72 hours. (A) Cell cycle analysis. At the end of treatment, cell cycle analysis was performed by flow cytometry as described in Materials and Methods. Representative DNA histograms of three independent experiments with similar results are shown. Cell cycle distribution was determined as described in Materials and Methods and shown on top of each histogram. (B) Apoptotic cell analysis. At the end of treatment, the cells were subjected to analysis of apoptosis using annexin V staining. Percentages of annexin V^+ cells were calculated. *$P < .05$, compared with control at each time point.

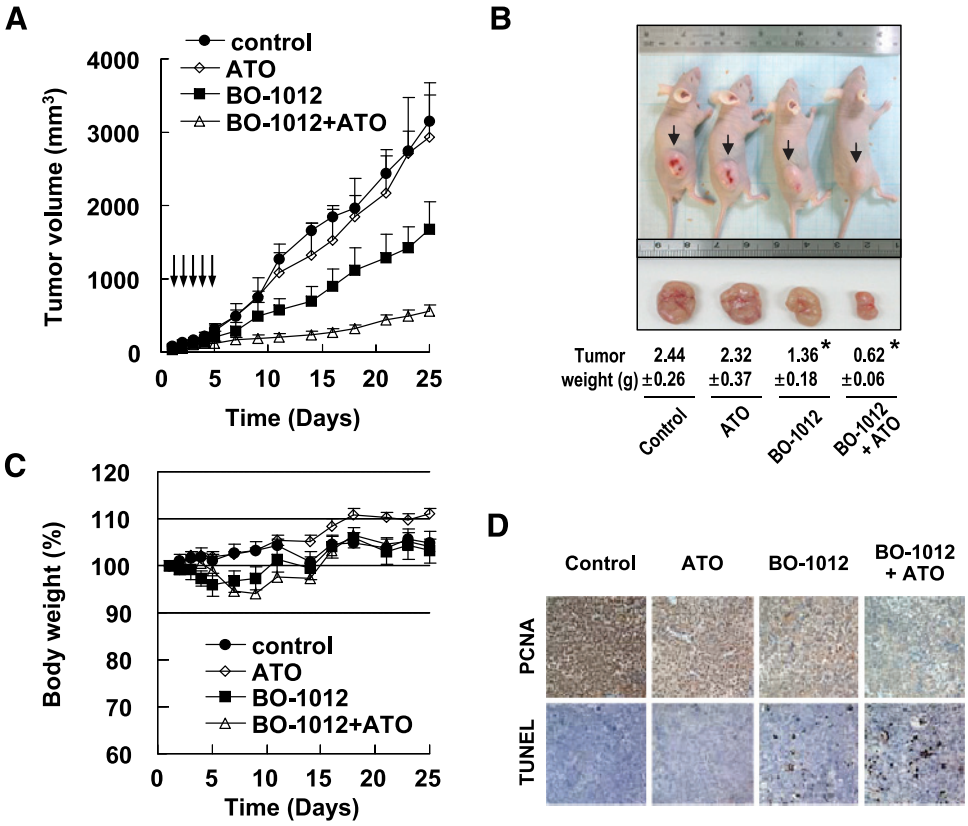

Figure 3. Synergistic anticancer activity of ATO and BO-1012 combination on the H460 xenograft. The nude mice with H460 xenograft were injected daily i.v. with 5 mg/kg ATO, 2.5 mg/kg BO-1012, or a combination of both agents for 5 days. (A) Tumor volumes. The numbers of animal in each group are six to seven. The tumor volumes were measured with calipers every 2 or 3 days, and these are expressed as mean ± SE. (B) Representative images of the mice bearing the tumors one the 25th day. The average tumor weights are shown at the bottom. *$P < .05$ compared with control. (C) Body weight change of mice. The body weights were measured every 2 or 3 days. (D) PCNA immunohistochemistry and TUNEL assay. Xenograft tumor sections from each group at 1 day after the last treatment (i.e., the sixth day after the first treatment) were taken out, sectioned, and subjected for PCNA immunohistochemistry and TUNEL assay as described in Materials and Methods.

ICLs (Figure 5*B*). The half-life of BO-1012–induced ICLs in H460 cells was ~26.2 hours in the absence of ATO but was ~82.7 hours in the presence of ATO. These results indicate that ATO is able to interfere with BO-1012–induced ICLs repair.

Because ICLs could result in DNA DSBs during DNA replication [37], we determined the effect of combining BO-1012 with ATO on the appearance of a DSB marker, phosphorylated histone H2AX (γH2AX) [38]. Immunofluorescence staining was adopted to examine the formation of γH2AX foci in nuclei (Figure 5, *C* and *D*). Image analysis showed that BO-1012 alone induced γH2AX nuclear foci at 48 hours, and the number of foci then declined at 72 hours; the percentages of cells with γH2AX foci were 36.5% and 25.9% at 48 and 72 hours, respectively, compared with 6.2% and 7.2% in untreated cells. Although BO-1012 treatment for 24 hours did not induce formation of γH2AX foci in nuclei (5.4%), a large amount of γH2AX was accumulated in the cytosol (Figure 5*C*), which is consistent with the increased number of γH2AX-positive cells detected at 24 hours by flow cytometry (Figure W3). ATO alone resulted in only a modest increase in γH2AX foci (26.8%). However, a large number of γH2AX nuclear foci were manifested at 24 hours in H460 cells treated with a combination of BO-1012 and ATO. The percentage of cells with γH2AX foci at 24 hours was more than 80% and declined only slightly at 72 hours (60.8%). These results indicate that ATO posttreatment enhanced the conversion of ICLs into DSBs, accelerated the recruitment of γH2AX in nuclei, and interfered with the repair of BO-1012–induced ICLs. Similar findings were observed by using flow cytometric analysis (Figure W3).

ATO Mediates through Inhibition of AKT to Interfere with Rad51-Associated Repair Activated by BO-1012

Because homologous recombination repair (HRR) and nonhomologous end-joining are two major repair pathways of DNA DSB, we therefore examined the nuclear translocation of Rad51 and DNA-PKcs, components of repair machineries of HRR and nonhomologous end-joining, respectively, in H460 cells treated with BO-1012, ATO, and in combination. As shown in Figure 6*A*, BO-1012 significantly induced translocation of Rad51 and DNA-PKcs to nucleus, whereas ATO alone did not affect the translocation of these two proteins. However, in BO-1012–treated cells, Rad51 accumulation in the nucleus was remarkably decreased by posttreatment with ATO, but DNA-PKcs accumulation in nucleus was not changed. We further confirmed the inhibitory effects of ATO on Rad51 activation by immunohistochemical technique (Figure 6*B*). Our results showed that BO-1012 resulted in substantially increased Rad51 foci in nuclei. Consistent to Western blot analysis, ATO alone did

not induce Rad51 foci in nucleus, but it did significantly reduce Rad51 foci in the nuclei of BO-1012–treated cells. These results indicated that BO-1012–induced damage could activate Rad51 and/or DNA-PKcs–associated repair machineries; however, ATO could inhibit Rad51 activation and, subsequently, enhance the anticancer effect of BO-1012.

Previous studies reported that the phosphoinositide 3-kinase (PI3K)–AKT signaling pathway modulates the expression or activation of Rad51 [39,40]. We therefore determined AKT activity in H460 cells treated with BO-1012, ATO, and in combination. As shown in Figure 6*C*, AKT was activated by BO-1012 by accumulation of pAKT, whereas combined treatment of BO-1012 and ATO significantly inhibited BO-1012–elicited AKT activity. To confirm the involvement of activated PI3K-AKT in BO-1012–triggered Rad51 activation, BO-1012–treated H460 cells were exposed to PI3K-AKT inhibitors, wortmannin, or AKTi. Our results showed that inhibition of AKT accompanied with decreased translocation of Rad51 into nuclei in BO-1012–treated cells (Figure 6*D*). These results suggest that ATO may mediate through the inhibition of AKT activity to interfere with Rad51 activation triggered by BO-1012.

Discussion

Either inherited or acquired resistance to chemotherapeutic drugs is a major limitation of therapy for cancer patients. A high capacity for DNA repair in cancer cells is frequently noted as one resistance mechanism [41]. In recent decades, novel therapeutic strategies and drug designs have been of great interest in cancer chemotherapy. The present study is the first to report a potent and a rational strategy for cancer

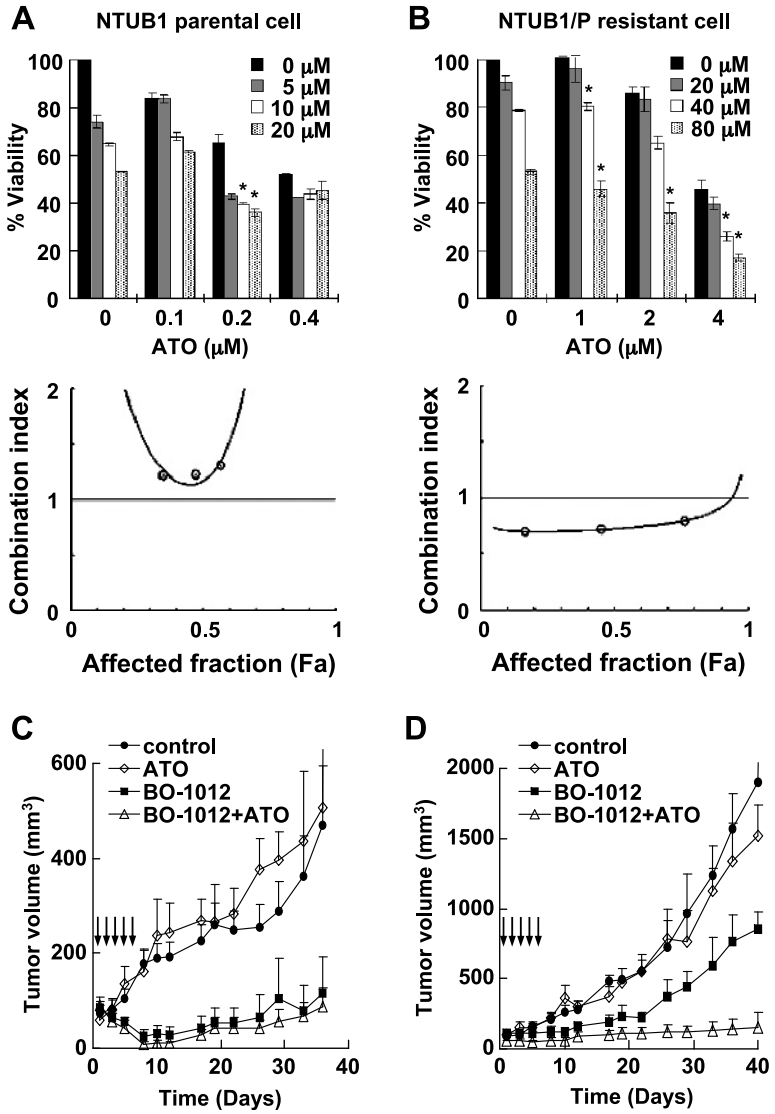

Figure 4. Synergistic anticancer activity of ATO and BO-1012 combination on human bladder cancer cells, NTUB1, and derived cisplatin-resistant NTUB1/P cells. (A and B) Cell viability analysis of BO-1012, ATO, and the combination of NTUB1 (A) and NTUB1/P (B) cells. Cell viability was assayed as described in Figure 1*B*. *$P < .05$ compared with ATO alone at each concentration. Bottom: The isobologram analysis of CI against affected fraction (Fa) was obtained by the constant-ratio combination method as described in Materials and Methods. (C and D) The anticancer activity of BO-1012, ATO, and in combination against NTUB1 (C) and NTUB1/P (D) tumors. The mice bearing NTUB1 or NTUB1/P xenografts were treated with individual drugs or in combination as described in Figure 3*A*. The numbers of animal in each group are four to six. The tumor volumes were measured with calipers at the indicated time points, and these are expressed as mean ± SE.

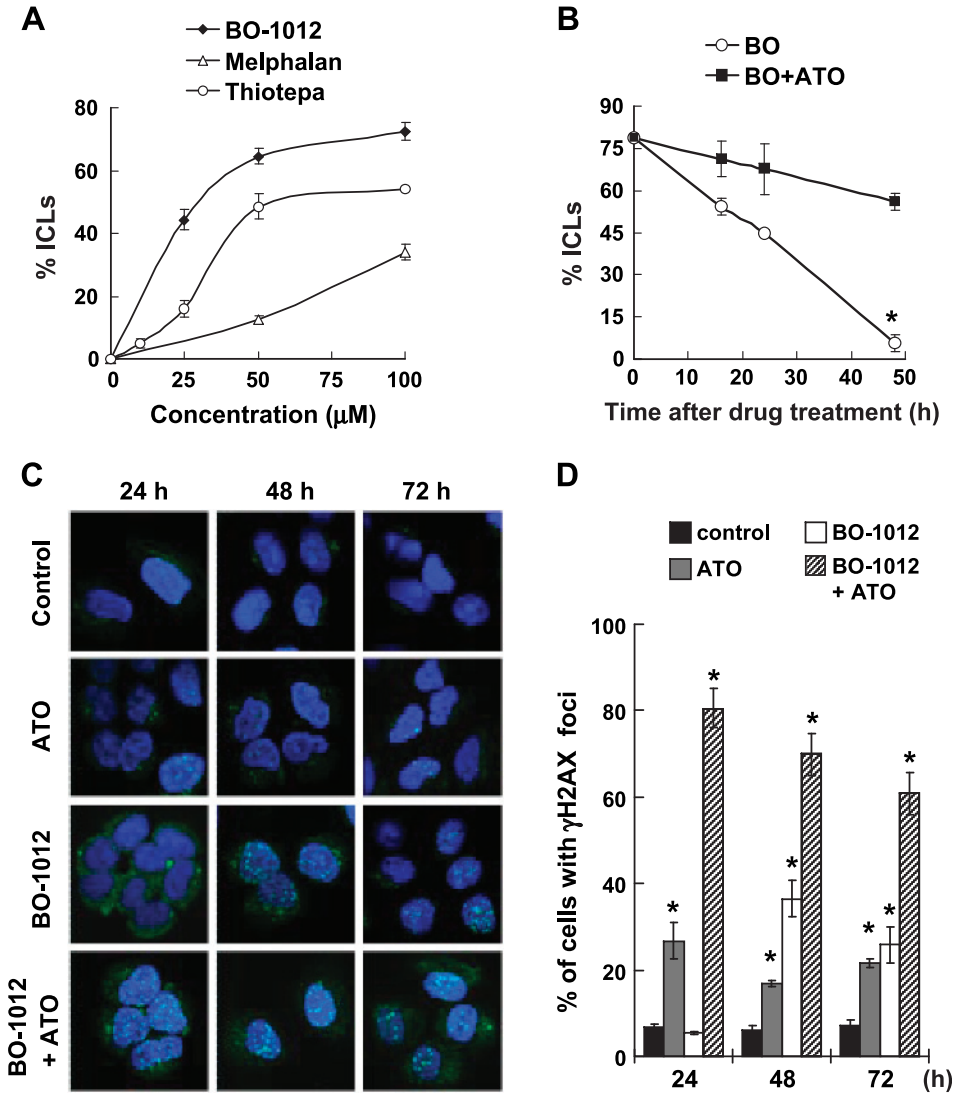

Figure 5. Inhibition of the repair of BO-1012 induced DNA damage and exaggeration of DSB formation by ATO. (A) Induction of ICLs by BO-1012, melphalan, and thiotepa. H460 cells were treated with various concentrations of BO-1012, melphalan, or thiotepa for 1 hour and then subjected for a modified comet assay as described in Materials and Methods. Percentage of DNA ICLs was calculated by the percentage of decrease in tail moment. (B) Inhibition of the repair of BO-1012–induced DNA ICLs by ATO. H460 cells were treated with 40 μM BO-1012 for 1 hour, washed, and then treated with 8 μM ATO for 16, 24, and 48 hours. *$P < .05$ compared with BO-1012 alone at the indicated time point. (C) Enhanced formation of BO-1012–induced γH2AX nuclei foci by ATO. H460 cells were treated with BO-1012, ATO, or in combination as described previously. After treatment, the detection of γH2AX (green) immunofluorescence staining was performed as described in Materials and Methods. Nuclei were counterstained with DAPI (blue). (D) The percentages of the cells containing four or more γH2AX nuclei foci were determined under a fluorescent microscope. *$P < .05$ compared with control at each time point.

therapy using a combination of BO-1012, a newly synthesized MMC derivative [11], with ATO, an agent that inhibits DNA repair. This drug combination strategy effectively suppressed the growth of H460 human large cell lung carcinoma in culture and in a xenograft mouse model compared with treatment with either agent alone. H460 cells were relatively resistant to several chemotherapeutic treatments, such as BO-1012, ATO, melphalan, and thiotepa (Figure 1), compared with other human solid tumors. Moreover, the therapeutic efficacy in mice bearing H460 xenografts is not convincing using conventional chemotherapy alone or in combination with ionizing radiation; although H460 tumor growth is inhibited during the drug-treated period, growth rapidly resumes after treatment [42,43]. H460 cells therefore provide an inherited resistant line for assessing efficacy of new treatments. In this study, we found that a combination of ATO and BO-1012 provided enhanced inhibition of tumor growth of H460 cells compared with BO-1012 alone.

In addition, we evaluated the effectiveness of this drug combination in cells with acquired cisplatin resistance. Platinum chemotherapies have become the most commonly prescribed chemotherapeutic drugs for treating solid cancers in patients [44]. Platinum resistance is a major clinical problem because there are no known drugs that can be used to circumvent this tumor resistance. We found that treatment with BO-1012 in combination with ATO was more effective in inhibiting the growth of an acquired cisplatin-resistant human bladder cancer, NTUB1/P, than was treatment with either single agent. Because the growth rate of NTUB1/P cells in nude mice was apparently faster than the parental NTUB1 cells, whether the growth rate playing certain roles on the synergism of BO-1012 and ATO remained to

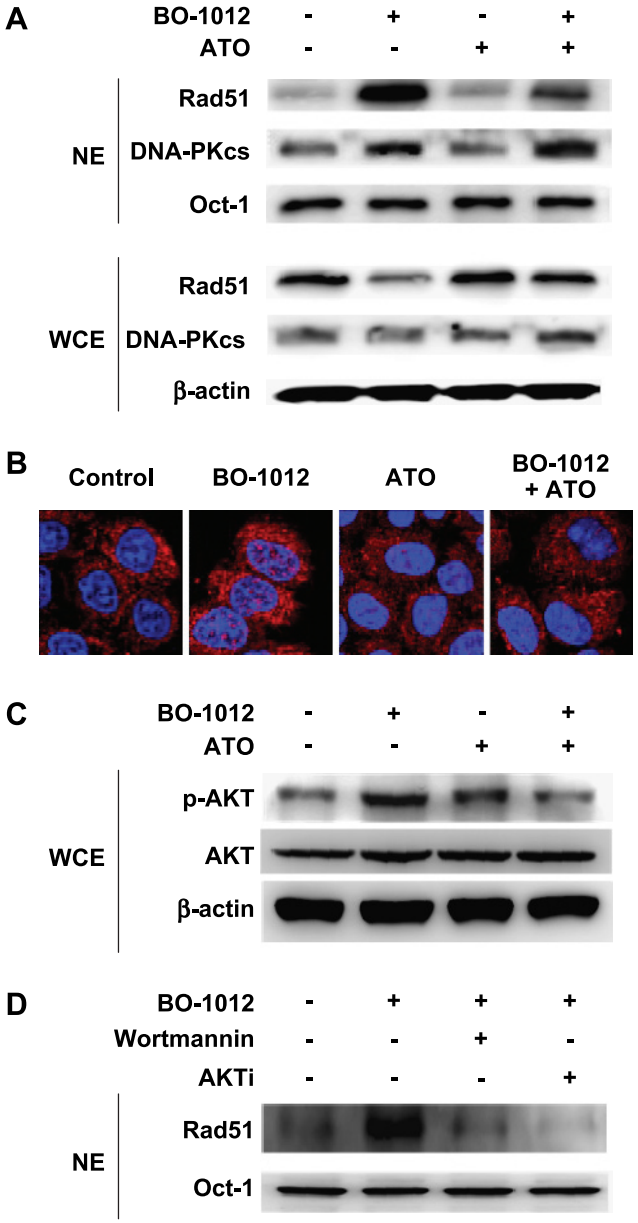

Figure 6. Inhibition of BO-1012–triggered Rad51 activation by ATO through decreased AKT activity. H460 cells were treated with 40 μM BO-1012 for 1 hour, washed, and then treated with 8 μM ATO for 24 hours. (A) Western blot analysis of Rad51 and DNA-PKcs in nuclear extracts (NE) and whole-cell extracts (WCE). At the end of treatment, an aliquot of NE and WCE were separated on a 10% SDS–polyacrylamide gel. Rad51 and DNA-PKcs were visualized by immunoblot analysis technique as described in Materials and Methods. Oct-1 and β-actin were included on the blot as loading controls for NE and WCE, respectively. (B) Immunofluorescence staining of Rad51. At the end of treatment, the cells were fixed and stained with primary antibody against Rad51 and then Alexa Fluor 555–conjugated secondary antibody (red) as described in Materials and Methods. Nuclei were counterstained with DAPI (blue). (C) Western blot analysis of AKT and pAKT. AKT and pAKT in WCE were analyzed as described in panel A using antibodies against AKT and p-AKT, respectively. (D) Inhibition of BO-1012 induced Rad51 translocation by wortmannin and AKTi. H460 cells were treated with 40 μM BO-1012 for 1 hour and followed with wortmannin (1 μM) or AKTi (20 μM) for 24 hours. After treatments, the nuclear extracts were subjected to Western blot analysis for Rad51 as described in Materials and Methods.

be clarified. Nevertheless, our study revealed that the combination of BO-1012 and ATO might be an effective regime for treatment of human cancer cells with inherited or acquired drug resistance.

A large number of synthetic and natural bifunctional alkylating agents exhibit anticancer activity because they can induce DNA ICLs [8,45]. The natural anticancer agent MMC and its analog(s) have been reported to cross-link to DNA double strands [46], and several synthetic bifunctional alkylating agents are under development [11]. The recently synthesized BO-1012 has been demonstrated to be a potent anticancer agent *in vitro* and in xenograft mouse models [11]. The mechanism of this agent's anticancer activity is thought to lie in the induction of DNA ICLs and further cellular responses. Once a replication fork stall or collapse is induced by treatment with bifunctional alkylating agents, repair pathways are required to recognize the problem and permit the resumption of replication. When collapsed replication forks are recognized, they trigger cell cycle arrest, DNA repair, or cell death through apoptosis [47]. In the present study, we confirmed that BO-1012 exerts its anticancer effect by inducing DNA ICLs, which may lead to DSBs, cell cycle arrest, and, finally, cell death. Compared with clinically used alkylating agents, melphalan and thiotepa, BO-1012 apparently induces a higher level of ICLs (Figures 5*A* and W3), and its combination with ATO exhibits potent anticancer activity.

Our present results demonstrate that DNA lesions induced by BO-1012 are still reparable, especially in relatively resistant cancer cells such as H460 cells. The efficacy of anticancer drugs is highly dependent on DNA repair capacity. Numerous studies have shown that cells defective in DNA repair exhibit sensitivity to cancer therapeutic agents such as etoposide, MMC, and ionizing radiation [48]. Unfortunately, a high degree of DNA repair activity is frequently observed in malignant cells, which results in resistance to chemotherapeutic drugs [48,49]. Inhibition of DNA repair activity is therefore a valuable strategy to enhance the efficacy of anticancer chemotherapeutics. A previous study has reported that resistance to O^6-alkylating agents can be overcome by depletion of a DNA repair protein, O^6-methylguanine-DNA methyltransferase [50]. In fact, DNA repair proteins are targets for anticancer drug development [51]. The combination of the DNA damaging agent temozolomide with inhibitors of O^6-methylguanine-DNA methyltransferase is currently under clinical trials [52]. Arsenic has been reported to impair base excision repair activity by down-regulation of DNA polymerase β (Pol β) and AP endonuclease [53] and to inhibit PARP-1 [54] and XPA [55] activity through competitive interaction with zinc. Our biochemical and immunological studies demonstrated that ATO could inhibit the activation of Rad51 in cells exposed to BO-1012.

Rad51 has been well documented to play a representative role on HRR-mediated DSB repair and cellular resistance to chemotherapies [56]. Functionally, when DNA DSB is formed by DNA-damaging agents, Rad51 interacted with chromatin and formed oligomers [56]. Several reports have shown that AKT may play important roles on modulation of Rad51-associated HRR [39,40]. In the present study, we demonstrated that AKT and Rad51 activations triggered by BO-1012 treatment were suppressed by ATO. These results suggest that ATO may mediate through the inhibition of AKT to interfere with DNA repair pathway, particularly Rad51-associated repair.

Emerging evidence has shown that ATO is an effective therapeutic for treatment of patients with relapse/refractory acute promyelocytic leukemia and multiple myeloma, with only mild adverse effects reported [12,57]. ATO-based chemotherapy is therefore a promising

treatment option for patients who tolerate or fail to respond to treatment with other chemotherapy regimens [57]. Because the high doses of ATO used for treatment of solid tumors are associated with clinical risks [58], the combination of ATO with other therapeutic agents may be a good strategy to reduce the ATO dose. In the present study, ATO at subtoxic doses was able to cooperate with BO-1012 to effectively suppress human solid tumor growth.

In the present study, we found that cell lines, such as H460, H1299, PC3, and NTUB1/P cells, that are more resistant to BO-1012 responded well to the addition of ATO, the combined treatment with BO-1012 and ATO and, therefore, may reveal a new clue for improving therapeutic efficacy of cancers with inherited or acquired drug resistance.

Acknowledgments

The authors thank Ling-Huei Yih for her critical review of the manuscript.

References

[1] Wadhwa PD, Zielske SP, Roth JC, Ballas CB, Bowman JE, and Gerson SL (2002). Cancer gene therapy: scientific basis. *Annu Rev Med* **53**, 437–452.

[2] Adair FE and Bagg HJ (1931). Experimental and clinical studies on the treatment of cancer by dichlorethylsulphide (mustard gas). *Ann Surg* **93**, 190–199.

[3] Musto P and D'Auria F (2007). Melphalan: old and new uses of a still master drug for multiple myeloma. *Expert Opin Investig Drugs* **16**, 1467–1487.

[4] La Rocca RV and Mehdorn HM (2009). Localized BCNU chemotherapy and the multimodal management of malignant glioma. *Curr Med Res Opin* **25**, 149–160.

[5] Ciurea SO and Andersson BS (2009). Busulfan in hematopoietic stem cell transplantation. *Biol Blood Marrow Transplant* **15**, 523–536.

[6] Valteau-Couanet D, Fillipini B, Benhamou E, Grill J, Kalifa C, Couanet D, Habrand JL, and Hartmann O (2005). High-dose busulfan and thiotepa followed by autologous stem cell transplantation (ASCT) in previously irradiated medulloblastoma patients: high toxicity and lack of efficacy. *Bone Marrow Transplant* **36**, 939–945.

[7] Knipp M (2009). Metallothioneins and platinum(II) anti-tumor compounds. *Curr Med Chem* **16**, 522–537.

[8] Hofheinz RD, Beyer U, Al-Batran SE, and Hartmann JT (2008). Mitomycin C in the treatment of gastrointestinal tumours: recent data and perspectives. *Onkologie* **31**, 271–281.

[9] McHugh PJ, Spanswick VJ, and Hartley JA (2001). Repair of DNA interstrand crosslinks: molecular mechanisms and clinical relevance. *Lancet Oncol* **2**, 483–490.

[10] Heckman JE, Lambert D, and Burke JM (2005). Photocrosslinking detects a compact, active structure of the hammerhead ribozyme. *Biochemistry* **44**, 4148–4156.

[11] Kakadiya R, Dong H, Lee PC, Kapuriya N, Zhang X, Chou TC, Lee TC, Kapuriya K, Shah A, and Su TL (2009). Potent antitumor bifunctional DNA alkylating agents, synthesis and biological activities of 3a-aza-cyclopenta[*a*] indenes. *Bioorg Med Chem* **17**, 5614–5626.

[12] Soignet SL, Frankel SR, Douer D, Tallman MS, Kantarjian H, Calleja E, Stone RM, Kalaycio M, Scheinberg DA, Steinherz P, et al. (2001). United States multicenter study of arsenic trioxide in relapsed acute promyelocytic leukemia. *J Clin Oncol* **19**, 3852–3860.

[13] Maeda H, Hori S, Nishitoh H, Ichijo H, Ogawa O, Kakehi Y, and Kakizuka A (2001). Tumor growth inhibition by arsenic trioxide (As_2O_3) in the orthotopic metastasis model of androgen-independent prostate cancer. *Cancer Res* **61**, 5432–5440.

[14] Kito M, Matsumoto K, Wada N, Sera K, Futatsugawa S, Naoe T, Nozawa Y, and Akao Y (2003). Antitumor effect of arsenic trioxide in murine xenograft model. *Cancer Sci* **94**, 1010–1014.

[15] Vuky J, Yu R, Schwartz L, and Motzer RJ (2002). Phase II trial of arsenic trioxide in patients with metastatic renal cell carcinoma. *Invest New Drugs* **20**, 327–330.

[16] Kim KB, Bedikian AY, Camacho LH, Papadopoulos NE, and McCullough C (2005). A phase II trial of arsenic trioxide in patients with metastatic melanoma. *Cancer* **104**, 1687–1692.

[17] Qian J, Qin S, and He Z (2001). Arsenic trioxide in the treatment of advanced primary liver and gallbladder cancer. *Zhonghua Zhong Liu Za Zhi* **23**, 487–489.

[18] Han YH, Kim SZ, Kim SH, and Park WH (2008). Induction of apoptosis in arsenic trioxide–treated lung cancer A549 cells by buthionine sulfoximine. *Mol Cells* **26**, 158–164.

[19] Lin YL, Ho IC, Su PF, and Lee TC (2006). Arsenite pretreatment enhances the cytotoxicity of mitomycin C in human cancer cell lines via increased NAD(P)H quinone oxidoreductase 1 expression. *Toxicol Appl Pharmacol* **214**, 309–317.

[20] Lee TC, Huang RY, and Jan KY (1985). Sodium arsenite enhances the cytotoxicity, clastogenicity, and 6-thioguanine–resistant mutagenicity of ultraviolet light in Chinese hamster ovary cells. *Mutat Res* **148**, 83–89.

[21] Wang W, Qin SK, Chen BA, and Chen HY (2001). Experimental study on antitumor effect of arsenic trioxide in combination with cisplatin or doxorubicin on hepatocellular carcinoma. *World J Gastroenterol* **7**, 702–705.

[22] Chun YJ, Park IC, Park MJ, Woo SH, Hong SI, Chung HY, Kim TH, Lee YS, Rhee CH, and Lee SJ (2002). Enhancement of radiation response in human cervical cancer cells *in vitro* and *in vivo* by arsenic trioxide (As_2O_3). *FEBS Lett* **519**, 195–200.

[23] Qazilbash MH, Saliba RM, Nieto Y, Parikh G, Pelosini M, Khan FB, Jones RB, Hosing C, Mendoza F, Weber DM, et al. (2008). Arsenic trioxide with ascorbic acid and high-dose melphalan: results of a phase II randomized trial. *Biol Blood Marrow Transplant* **14**, 1401–1407.

[24] Campbell RA, Sanchez E, Steinberg JA, Baritaki S, Gordon M, Wang C, Shalitin D, Chen H, Pang S, Bonavida B, et al. (2007). Antimyeloma effects of arsenic trioxide are enhanced by melphalan, bortezomib and ascorbic acid. *Br J Haematol* **138**, 467–478.

[25] Ning S and Knox SJ (2006). Optimization of combination therapy of arsenic trioxide and fractionated radiotherapy for malignant glioma. *Int J Radiat Oncol Biol Phys* **65**, 493–498.

[26] Lee TC, Kao SL, and Yih LH (1991). Suppression of sodium arsenite–potentiated cytotoxicity of ultraviolet light by cycloheximide in Chinese hamster ovary cells. *Arch Toxicol* **65**, 640–645.

[27] Walter I, Schwerdtle T, Thuy C, Parsons JL, Dianov GL, and Hartwig A (2007). Impact of arsenite and its methylated metabolites on PARP-1 activity, PARP-1 gene expression and poly(ADP-ribosyl)ation in cultured human cells. *DNA Repair (Amst)* **6**, 61–70.

[28] Andrew AS, Burgess JL, Meza MM, Demidenko E, Waugh MG, Hamilton JW, and Karagas MR (2006). Arsenic exposure is associated with decreased DNA repair *in vitro* and in individuals exposed to drinking water arsenic. *Environ Health Perspect* **114**, 1193–1198.

[29] Hartwig A, Blessing H, Schwerdtle T, and Walter I (2003). Modulation of DNA repair processes by arsenic and selenium compounds. *Toxicology* **193**, 161–169.

[30] Lai KC, Chang KW, Liu CJ, Kao SY, and Lee TC (2008). IFN-induced protein with tetratricopeptide repeats 2 inhibits migration activity and increases survival of oral squamous cell carcinoma. *Mol Cancer Res* **6**, 1431–1439.

[31] Yu HJ, Tsai TC, Hsieh TS, and Chiu TY (1992). Characterization of a newly established human bladder carcinoma cell line, NTUB1. *J Formos Med Assoc* **91**, 608–613.

[32] Pu YS, Hour TC, Chen J, Huang CY, Guan JY, and Lu SH (2002). Cytotoxicity of arsenic trioxide to transitional carcinoma cells. *Urology* **60**, 346–350.

[33] Chou TC (2006). Theoretical basis, experimental design, and computerized simulation of synergism and antagonism in drug combination studies. *Pharmacol Rev* **58**, 621–681.

[34] Chou TC (2010). Drug combination studies and their synergy quantification using the Chou-Talalay method. *Cancer Res* **70**, 440–446.

[35] Yih LH, Tseng YY, Wu YC, and Lee TC (2006). Induction of centrosome amplification during arsenite-induced mitotic arrest in CGL-2 cells. *Cancer Res* **66**, 2098–2106.

[36] Kang YH, Yi MJ, Kim MJ, Park MT, Bae S, Kang CM, Cho CK, Park IC, Park MJ, Rhee CH, et al. (2004). Caspase-independent cell death by arsenic trioxide in human cervical cancer cells: reactive oxygen species–mediated poly(ADP-ribose) polymerase-1 activation signals apoptosis-inducing factor release from mitochondria. *Cancer Res* **64**, 8960–8967.

[37] Lopes M, Cotta-Ramusino C, Pellicioli A, Liberi G, Plevani P, Muzi-Falconi M, Newlon CS, and Foiani M (2001). The DNA replication checkpoint response stabilizes stalled replication forks. *Nature* **412**, 557–561.

[38] Fernandez-Capetillo O, Allis CD, and Nussenzweig A (2004). Phosphorylation of histone H2B at DNA double-strand breaks. *J Exp Med* **199**, 1671–1677.

[39] Ko JC, Ciou SC, Jhan JY, Cheng CM, Su YJ, Chuang SM, Lin ST, Chang CC, and Lin YW (2009). Roles of MKK1/2–ERK1/2 and phosphoinositide 3-kinase–AKT signaling pathways in erlotinib-induced Rad51 suppression and cytotoxicity in human non–small cell lung cancer cells. *Mol Cancer Res* **7**, 1378–1389.

[40] Plo I, Laulier C, Gauthier L, Lebrun F, Calvo F, and Lopez BS (2008). AKT1 inhibits homologous recombination by inducing cytoplasmic retention of BRCA1 and RAD51. *Cancer Res* **68**, 9404–9412.

[41] Miyagawa K (2008). Clinical relevance of the homologous recombination machinery in cancer therapy. *Cancer Sci* **99**, 187–194.

[42] Carter CA, Chen C, Brink C, Vincent P, Maxuitenko YY, Gilbert KS, Waud WR, and Zhang X (2007). Sorafenib is efficacious and tolerated in combination with cytotoxic or cytostatic agents in preclinical models of human non–small cell lung carcinoma. *Cancer Chemother Pharmacol* **59**, 183–195.

[43] Amorino GP, Mohr PJ, Hercules SK, Pyo H, and Choy H (2000). Combined effects of the orally active cisplatin analog, JM216, and radiation in antitumor therapy. *Cancer Chemother Pharmacol* **46**, 423–426.

[44] Cossa G, Gatti L, Zunino F, and Perego P (2009). Strategies to improve the efficacy of platinum compounds. *Curr Med Chem* **16**, 2355–2365.

[45] Tomasz M and Palom Y (1997). The mitomycin bioreductive antitumor agents: cross-linking and alkylation of DNA as the molecular basis of their activity. *Pharmacol Ther* **76**, 73–87.

[46] Plumb JA and Workman P (1994). Unusually marked hypoxic sensitization to indoloquinone EO9 and mitomycin C in a human colon–tumour cell line that lacks DT-diaphorase activity. *Int J Cancer* **56**, 134–139.

[47] Sorensen CS, Hansen LT, Dziegielewski J, Syljuasen RG, Lundin C, Bartek J, and Helleday T (2005). The cell-cycle checkpoint kinase Chk1 is required for mammalian homologous recombination repair. *Nat Cell Biol* **7**, 195–201.

[48] Darzynkiewicz Z, Traganos F, and Wlodkowic D (2009). Impaired DNA damage response—an Achilles' heel sensitizing cancer to chemotherapy and radiotherapy. *Eur J Pharmacol* **625**, 143–150.

[49] Chabner BA and Roberts TG Jr (2005). Timeline: chemotherapy and the war on cancer. *Nat Rev Cancer* **5**, 65–72.

[50] Gerson SL, Berger NA, Arce C, Petzold SJ, and Willson JK (1992). Modulation of nitrosourea resistance in human colon cancer by O^6-methylguanine. *Biochem Pharmacol* **43**, 1101–1107.

[51] Helleday T, Petermann E, Lundin C, Hodgson B, and Sharma RA (2008). DNA repair pathways as targets for cancer therapy. *Nat Rev Cancer* **8**, 193–204.

[52] Quinn JA, Jiang SX, Reardon DA, Desjardins A, Vredenburgh JJ, Gururangan S, Sampson JH, McLendon RE, Herndon JE II, and Friedman HS (2009). Phase 1 trial of temozolomide plus irinotecan plus O^6-benzylguanine in adults with recurrent malignant glioma. *Cancer* **115**, 2964–2970.

[53] Sykora P and Snow ET (2008). Modulation of DNA polymerase β-dependent base excision repair in cultured human cells after low dose exposure to arsenite. *Toxicol Appl Pharmacol* **228**, 385–394.

[54] Qin XJ, Hudson LG, Liu W, Timmins GS, and Liu KJ (2008). Low concentration of arsenite exacerbates UVR-induced DNA strand breaks by inhibiting PARP-1 activity. *Toxicol Appl Pharmacol* **232**, 41–50.

[55] Mustra DJ, Warren AJ, Wilcox DE, and Hamilton JW (2007). Preferential binding of human XPA to the mitomycin C–DNA interstrand crosslink and modulation by arsenic and cadmium. *Chem Biol Interact* **168**, 159–168.

[56] Daboussi F, Dumay A, Delacote F, and Lopez BS (2002). DNA double-strand break repair signalling: the case of RAD51 post-translational regulation. *Cell Signal* **14**, 969–975.

[57] Berenson JR and Yeh HS (2006). Arsenic compounds in the treatment of multiple myeloma: a new role for a historical remedy. *Clin Lymphoma Myeloma* **7**, 192–198.

[58] Westervelt P, Brown RA, Adkins DR, Khoury H, Curtin P, Hurd D, Luger SM, Ma MK, Ley TJ, and DiPersio JF (2001). Sudden death among patients with acute promyelocytic leukemia treated with arsenic trioxide. *Blood* **98**, 266–271.

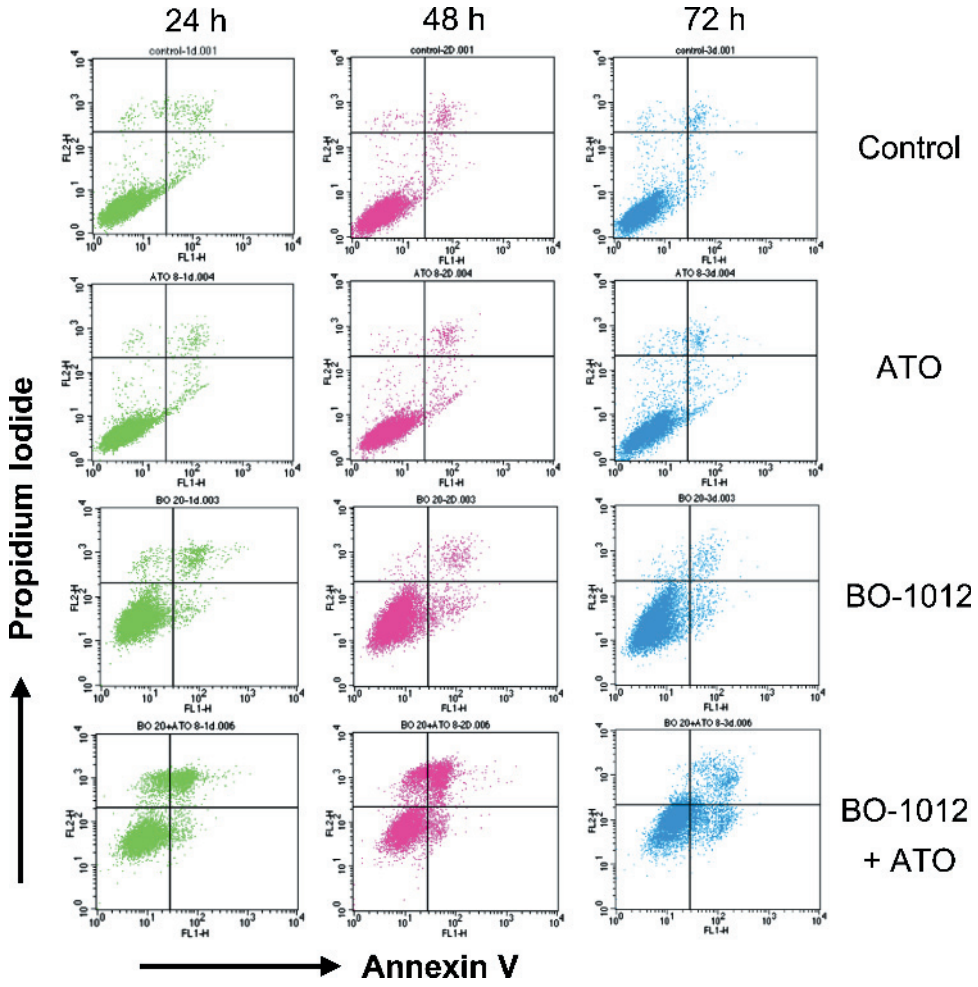

Figure W1. Apoptotic cell death induced by BO-1012, ATO, and in combination. H460 cells were treated with 20 μM BO-1012 for 1 hour, washed, and then treated with 8 μM ATO for 24, 48, or 72 hours. After treatment, the cells were subjected to analysis of apoptosis using annexin V staining. Representative flow cytometry analysis of apoptotic cell death.

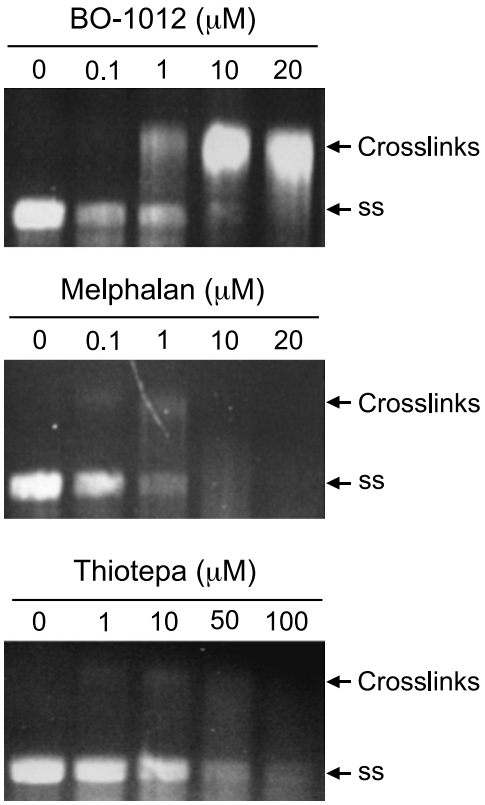

Figure W2. Formation of DNA ICLs by BO-1012, melphalan, and thiotepa. pEGFP-N1 plasmid DNA was incubated with various concentrations of drugs. At the end of treatment, the DNA ICLs were analyzed by alkaline gel shift assay as described in Materials and Methods. *ss* indicates single-strand DNA; *cross-links*, DNA ICLs.

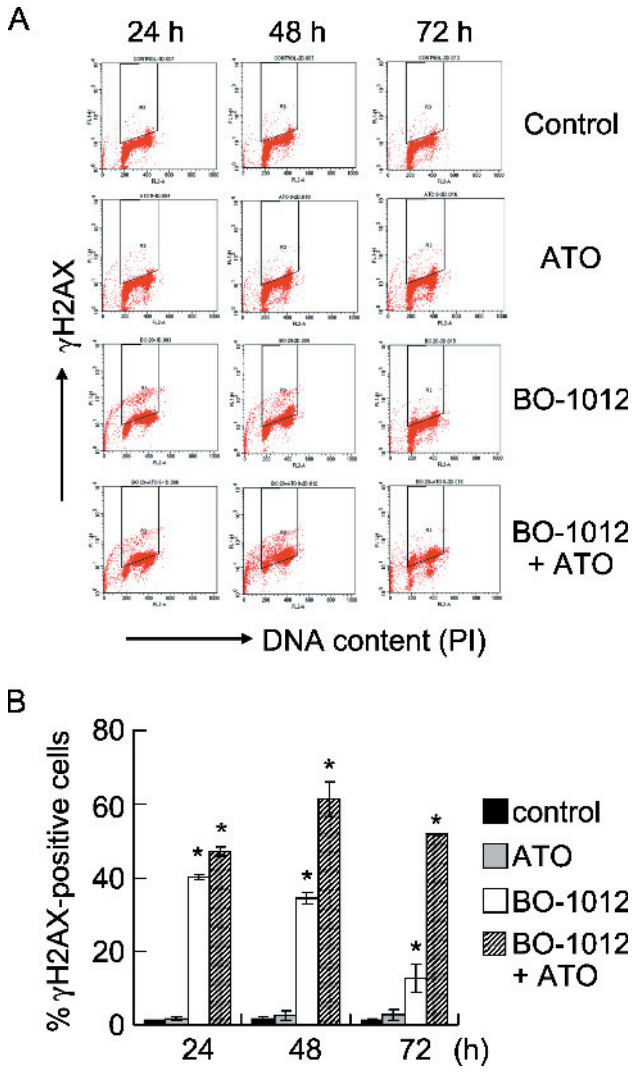

Figure W3. Enhancement of histone H2AX phosphorylation by BO-1012, ATO, and in combination. H460 cells were treated with 20 μM BO-1012 for 1 hour, washed, and then treated with 8 μM ATO for 24, 48, or 72 hours. (A) Flow cytometric analysis of γH2AX. After treatment, flow cytometry analysis of γH2AX was performed as described in Materials and Methods. (B) Percentage of γH2AX-positive cells. The γH2AX-positive cells in the rectangle of each dot plot (A) were gated.